Centrifuge 88, Corté (ed.)

The design of deep in-situ walls

M.D.Bolton & D.I.Stewart
Cambridge University, London, UK
W.Powrie
University of London, King's College, UK

ABSTRACT: Twenty-two centrifuge model tests have been used to explore both collapse mechanisms and soil-wall deformation patterns of diaphragm walls in overconsolidated clay. A variety of collapse mechanisms was observed which could be back-analysed with reasonable success using classical methods. In addition, the behaviour of walls which did not collapse outright was sufficiently coherently observed to permit the proposal of a straightforward design method based on a serviceability criterion.

The permissible wall displacement can be converted to a mobilised soil strain through the agency of an appropriate simplified strain field. The mobilised strain is related to a mobilised soil strength by means of standard element tests. This mobilised strength can then be used to derive earth pressure coefficients for an equilibrium analysis of the wall, leading to the selection of a wall penetration and the calculation of bending moments and propping forces under working conditions.

1. INTRODUCTION

Recent advances in construction technology, together with the high cost of city centre building land, have led to the increasing use of in situ retaining walls in connection with motorways and deep basements in urban areas. In many cases, the retained soil will be a clay, and existing codes of practice offer little guidance to the designer of a wall retaining such a soil. One of the principal uncertainties concerns the behaviour of the wall as the groundwater regime moves towards its long term equilibrium state.

The excess pore water suctions induced in the retained soil on excavation in front of the wall can take years or even decades to dissipate. In a 1:n scale model this time is reduced by a factor of n^2, thus a model test represents the only method by which the long-term behaviour of a geotechnical construction in a soil of low permeability may be observed over a reasonably short period of time.

A series of model tests has been conducted using the Cambridge Geotechnical Centrifuge (Schofield 1980) as part of an investigation into the behaviour of diaphragm walls in clay (Powrie 1986). This paper is concerned principally with the application of the centrifuge test results to the design of deep in situ walls of this type.

2. THE DESIGN OF THE CENTRIFUGE MODEL

A typical centrifuge model is illustrated in Figure 1, and represents a section of a long retaining wall. The length of the model wall section was 150mm, corresponding to 18.75m of a prototype wall at a scale of 1:125. It was decided that, for ease of back-analysis, the deformation should take place under conditions of plane strain. The plane vertical boundaries perpendicular to the face of the model wall should therefore ideally have been rigid and frictionless. The centrifuge strongbox designed for the model tests had a 16mm thick dural backplate with two horizontal stiffening beams, and an 80mm thick perspex front window. In order to reduce friction to a minimum, the inside of the backplate was well-lubricated with Molykote 33

silicone grease, and the inside of the perspex window was sprayed with a mould release agent, Adsil, so that the view of the model was not obscured. It is estimated that the total restraining force due to friction from all sources would be less than 10% of the typical fully active force (including pore water pressure) acting on the retained side of the model wall above excavation level.

The clay used in the model tests was speswhite kaolin, chosen principally because of its relatively high permeability $k=0.8\times10^{-9}$ m/s (Al Tabbaa 1987). Kaolin powder was mixed under a partial vacuum with de-ionised water to a slurry with a moisture content of 120% (about twice the liquid limit). The slurry was then poured into a consolidation press, where it was gradually compressed one-dimensionally to a vertical effective stress of 1250 kN/m^2, and then unloaded to a vertical effective stress of 80kN/m^2.

At an average effective stress of about 100kN/m^2, the clay was removed from the consolidation press and cut to receive the model retaining wall. The excavation was also made at this stage. The clay removed was replaced by a rubber bag containing zinc chloride solution, mixed to the same unit weight as the clay and filled to the level of the retained ground. The model was then transferred to the centrifuge strongbox and instrumented. After an initial reconsolidation period, during which the clay sample comes into equilibrium at 125g under its enhanced self weight, the profile of overconsolidation ratio based on vertical effective stresses corresponds to the removal by erosion of about 150m of overlying soil and represents the conditions which would prevail in a typical overconsolidated clay deposit.

The horizontal earth pressures require further consideration. Although the in situ lateral earth stresses in an overconsolidated clay deposit are likely to be high, the slurry trench phase of diaphragm wall construction is certain to alter them significantly. The exact effect of the casting of the wall will depend on the relative time-scales of wall construction and excess pore water pressure dissipation in the soil, the unit weight of the bentonite slurry, the unit weight of the concrete, and the rapidity with which the concrete sets. An approximate analysis can be used to estimate limits to the likely pre-excavation lateral earth pressure coefficient (Powrie 1985). In London clay, for example, the slurry trench phase might reduce an initial effective earth pressure coefficient of 2.0 to between 1.0 and 1.2. A pre-excavation lateral earth pressure coefficient of unity was therefore considered appropriate for the model diaphragm wall tests.

Recalling that the zinc chloride solution was mixed to the same unit weight as the soil it replaced, the boundary stresses were approximately consistent with this requirement after reconsolidation in the centrifuge. The establishment of Ko=1 in the heavy fluid need not, of course, imply that Ko was exactly unity either behind the stiff wall or beneath the floor of the excavation, especially if the wall were propped. Bending moments measured in more flexible walls during the reconsolidation phase indicated that Ko = 1 was quite closely achieved behind these walls, which were of similar stiffness to practical prototypes.

It is sometimes difficult to monitor in sufficient detail the changes in state which occur when construction processes are modelled in the centrifuge. In these circumstances a finite element analysis of the process may prove useful. Figure 2 shows that the pre-"excavation" lateral earth pressures predicted by White (1987) for the wall propped at the crest, using CRISP with a Cam clay soil model are reasonably close to those given by the Ko=1 approximation.

The model therefore generates an artificial initial condition with pore water pressures in approximate equilibrium with a high groundwater table, and with Ko approximately equal to unity. The provision of a valve-operated waste pipe then enables the zinc chloride solution to be drained from the rubber bag to simulate the excavation of the soil in front of the wall. As the fluid is drained, the lateral pressure reduction is proportional to the drop in level. A stress path with little initial horizontal stress reduction would apply beneath a real soil excavation: the transient process is thus modelled only approximately. Since the stress boundary conditions are correct both before and after excavation, and the time taken to drain the zinc chloride solution is comparatively short (2 to 5 minutes at model scale, corresponding to 3 to 8 weeks at prototype scale for a 10m retained height), it is considered that the error introduced is negligible.

The layout of a typical model with its instrumentation is shown in Figure 3. In all tests, the retained height of 80mm in the model represented 10m at prototype scale. The model walls were intended to be impermeable to groundwater and effectively rigid in bending. They were made of either 9.5mm or 4.7mm dural plate, giving equivalent bending stiffnesses (EI) at prototype scale of approximately 10^7 and 1.2×10^6 kNm^2 per metre. The faces of the model walls were covered with a 2mm thick coating of resin to protect the strain gauges and wires and to achieve a uniform and repeatable surface finish. The angle of friction between the resin and kaolin was investigated by inserting a coated plate of aluminium in a shear box, with the surface of the resin flush with the plane of shearing. An effective angle $\delta = 21.1°$ was recorded after about 1.5mm of box displacement, dropping to 18.3° after a further 2.5mm. It is consistent with the concept of critical states to infer that a surface upon which there was an insignificant opportunity for dilation, but whose roughness was comparable with the particle size, might mobilise $\delta = \phi_{crit}$. Such a surface might, as with other rupture surfaces, provide an opportunity for sliding leading to the development of residual friction conditions. For the purposes of back-analysis δ was not permitted to exceed $\phi_{crit}=22°$ (Al Tabbaa 1987; Sketchley 1973).

Peak angles of shearing resistance were determined for samples of kaolin taken through a sequence of preconsolidation and trimming identical to that experienced by the soil in the model. In undrained tests starting from an OCR of about 10, which corresponds to the mid-height of the centrifuge model, ϕ'_{max} was found to be in the range 21° to 25° (secant values) in both triaxial and plane compression tests which failed by the formation of a rupture surface. A drained triaxial compression test failed at $\phi_{max}=26°$, and this value was used as an upper bound for the purposes of back-analysis.

In most tests, a full height groundwater level on the retained side of the wall was modelled and special silicone rubber wiper-seals were used to prevent water from leaking between the edges of the wall and the sides of the strongbox. Standpipes with overflow outlets at fixed elevations were supplied with water from hydraulic slip rings to create constant head devices. By adjusting the supply flowrate, the elevation of water above the standpipe outlet could be finely adjusted. During the initial re-consolidation, water was supplied at the elevation of the ground surface to each of: the ground surface, the base drainage sheet, and the floor of the excavation. After "excavation", solenoid valves were used to switch drainage lines so as to isolate the base drain and to keep the water level in the excavation drawn down to its floor. It can be shown that the presence of the isolated drainage sheet at the base of the model causes the steady seepage solution to mimic that of a much deeper soil stratum.

In all, twenty two model tests were used to explore both collapse mechanisms and soil-wall deformation patterns. Walls were either simple embedded cantilevers or were propped at the crest or the level of the excavation but in all cases they modelled a retained height of 10m of clay.

A variety of collapse mechanisms was observed which could be back-analysed with reasonable success using classical methods., Well-known phenomena such as the damaging effect of free water entering a tension crack were observed. These results and analyses have been reported elsewhere (Bolton & Powrie 1987).

In some tests, the depth of embedment of the model wall was sufficient to prevent collapse. In these cases, measurements of pore water pressures, soil displacements and wall bending moments were sufficiently coherent to permit the proposal of a straightforward design method based on a serviceability criterion.

3. AN UNPROPPED WALL

Centrifuge test DWC08 featured an unpropped wall of 10m retained height,

20m embedment and a bending stiffness of 10^7kNm²/m, with a water table initially at the ground surface. This wall was at first apparently stable, but gradually suffered increasing deformation as the pore water suctions induced on excavation dissipated and steady-state seepage was approached. This is illustrated by Figure 4 which records the displacement at the crest as a function of time at prototype scale.

The equilibrium of an embedded cantilever is usually analysed using a "fixed earth support" method which invokes a hypothetical force at the toe. Figure 5 shows an alternative stress analysis with Rankine zones of active and passive pressure switching around a "pivot" close to the toe. Distributions such as these were found to be reasonably accurate in their back analysis of limiting stability. For example, taking pore pressure data and excavation dimensions corresponding to the end of test DWC08, equilibrium is achieved using earth pressure coefficients following Caquot and Kerisel if $\phi'=24°$, $\delta = 22°$. It is entirely reasonable to expect that limiting strengths such as these should have been mobilised after 1.1m of (prototype) crest deflection and 7% soil shear strain.

It will now be assumed that stress distributions of this type are of relevance not only at collapse, but also in the phase of increasing strain prior to collapse. In other words, if a particular wall would be in limiting equilibrium with earth pressure coefficients corresponding to $\phi'=20°$ in certain zones it will be assumed that the soil in these zones will uniformly mobilise 20° of its available angle of shearing even if that were to be somewhat larger, say 26°, so that the wall was not on the point of failure. At first sight such an assumption might seem unpromising. However, equilibrium is the essential condition leading to the selection of a value of mobilised strength. Only if the shape of the stress distribution prior to collapse were substantially different to that at failure would the assumption lead to significant error.

Figure 6 shows the soil displacements (measured from films) which occurred during excavation in test DWC08. The boundaries of significant soil displacement may reasonably be represented by lines at 45° extending upward on each side of the wall from a point near the toe. Figure 7 shows a simple theoretical strain field, derived after Bransby and Milligan (1975) and adapted to the deformation of an embedded cantilever. The direction of principal compressive strain increment switches between vertical and horizontal around a pivot O, in harmony with the assumed stress distributions.

It should be noted that strict internal consistency within and between these equilibrium and kinematic assumptions is restricted to the case of zero wall friction and the assumption that the horizontal plane through the pivot is also frictionless. However, Bransby and Milligan showed that wall roughness had a negligible effect on the strain fields observed in model tests with sand, and that dilatancy also had a negligible effect on the relationship between soil strain $\delta\gamma$ and wall rotation $\delta\theta$. The idealisation of figure 7 offers the result that $\delta\gamma=2\delta\theta$ in all zones adjacent to the wall, while it is taken to be zero elsewhere.

Stress analysis following Figure 5 leads to the calculation of a mobilised angle of shearing which is required for equilibrium. Strain analysis following figure 7 permits the wall rotation to be calculated if the soil shear strain is known. The linkage between mobilized stress and strain can be provided by an appropriate test on a representative soil element, such as the plane strain test shown in Figure 8. It is then possible to back analyse a particular wall configuration to test the hypotheses outlined above.

The wall geometry and pore water pressure distribution immediately after "excavation" in test DWC08 were used in a stress analysis after the fashion of Figure 5 to deduce a mobilised angle of shearing $\phi'=\delta=17.5°$ (assuming full wall friction). The corresponding shear strain increment according to Figure 8 is 1.1%. The compatible wall rotation according to Figure 7 would be 0.55% which would create a crest deflection of 158mm (prototype scale). This can be compared in Figure 4 with the observed deflection of 170mm shortly after the completion of the excavation process. The concomitant soil deflections are shown in Figure 9, and these can be compared with the observations shown in Figure 6.

4. A WALL PROPPED AT THE CREST

The model wall used in test DWC16 was propped at the crest with a retained height of 10m, a depth of embedment of 15m and a bending stiffness of 1.2×10^6kNm²/m - all at prototype scale. Two props were used with a horizontal separation of 50mm: each was strain-gauged to record thrust. The wall itself was strain-gauged to record bending moments and these are shown as functions of time in Figure 10a. The gradual increase in the bending moments is directly attributable to the readjustment of pore water pressures to their long-term equilibrium values, and in particular to the dissipation of the excess pore water suctions induced in the soil on excavation (Figure 10b).

The pore water pressures measured near the model wall at two instants during the test are recorded in Figure 11a and compared with those before excavation. The first instant was shortly after excavation, and the second instant was near the end of the test after 12.3 years would have elapsed at prototype scale and steady seepage established. The idealised linear pore water pressure distributions shown in Figure 11a were used in the back-analysis of the model test. In Figure 11b, the pore water pressures measured after 12.3 years at prototype scale are compared with the values obtained from a steady-state seepage flownet.

The bending moments measured in the model wall at these two instants during the test are shown - at prototype scale - in Figure 12, together with the corresponding prop forces. Computed bending moment diagrams are also shown: these were calculated on the assumption that the effective lateral earth pressure is proportional to the depth below the soil surface, and that the wall is perfectly rough - that is, $\delta=\phi'_{mob}$. For a wall propped at the crest, an admissible strain field is shown in Figure 13 which indicates that, for a given wall rotation θ, the maximum shear strain on the retained side is 2θ, and that on the excavated side is $2\theta\left(1+\frac{h}{d}\right)$. In this case, h=10m and d=15m, and the maximum shear strain on the excavated side is a factor of 5/3 greater than that on the retained side. The idealised effective stress distributions are typified in Figure 14. The moment equilibrium calculation for the earth pressure coefficients K_1 (on the retained side) and K_2 (on the excavated side) was repeated until a pair of values was found corresponding to mobilised angles of shearing on each side of the wall which would be consistent, according to the laboratory test data, Figure 8, with this difference in characteristic shear strain. The measured pore water pressures were introduced into the calculation by means of the linear idealisations shown in Figure 11a. The prop load was then obtained from the condition of horizontal equilibrium, and the bending moments were calculated from the loads on the wall in the normal way.

Figure 12 shows that the bending moments measured just after excavation in test DWC16 are close to those calculated using this method with $K_1=0.57$ and $K_2=2.22$, which correspond to $\delta=\phi'=12.5°$ and $\gamma=0.5\%$ on the retained side, and $\delta=\phi'=15.9°$ and $\gamma=0.8\%$ on the excavated side of the wall. After 12.3 years at prototype scale, the measured bending moments are close to those calculated using $K_1=0.55$ ($\delta=\phi'=13.5°$, $\gamma=0.55\%$) and $K_2=2.35$ ($\delta=\phi'=16.8°$, $\gamma=0.95\%$). The measured and computed prop loads are also in reasonable agreement.

Figure 15 shows the soil displacements - measured from films - which occurred during excavation. It may be noted that the horizontal movement of the retained soil near the top of the wall was larger than would be expected for a wall propped rigidly at its crest. This was due to a lack of contact between the wall and the props at the start of the excavation process. Whilst every care was taken to ensure that the props were initially correctly placed, no control could be exercised over relative movements between the wall and the props during reconsolidation in the centrifuge. During excavation, the top of the wall moved forwards by just under 0.6mm, which corresponds to about 70mm at prototype scale. The effect of this lack of fit is not taken into account by the admissible strain field shown in Figure 13. Therefore, the displacements measured in centrifuge test DWC14, on a wall of similar geometry but with a bending stiffness at prototype scale of

10^7kNm²/m which was rigidly propped at the crest, will be compared with those calculated using the equilibrium calculation and admissible strain field already described.

According to the stress field analysis shown in Figure 14, the wall of test DWC14 would be in equilibrium with the pore water pressures measured immediately after excavation and soil stresses given by earth pressure coefficients K_1=0.47 and K_2=2.85. These coefficients correspond to $\delta=\phi'=17.25°$ and γ=1.05% on the retained side, and $\delta=\phi'=20.1°$ and γ=1.72% on the excavated side of the wall.

The measured and calculated soil settlements are compared in Figure 16. Although the maximum surface displacements are of the same order, the detailed strain distribution is not well represented in this case by the idealised strain field of Figure 13.

The methods used for the back-analysis of events which had already occurred can be applied to design, but the approach would differ slightly in two respects.

1. Depending on the pre-excavation soil stresses and the proposed method of construction, it might be more appropriate to invoke a different relationship between the angles of soil friction on each side of the wall. This would be based on in situ test data for K_0 and laboratory test data for ϕ' as a function of shear strain.

2. For an effective stress analysis, pore water pressures must be predicted. The transient pore water suctions induced on excavation are a function of the structural stiffness. If the soil can be assumed to be isotropic and reversibly elastic, the transient pore water pressures can be estimated from the condition that p'=constant. The long term pore water pressures are dominated by seepage, and are therefore a function of geometry and not of structural stiffness: they can be estimated easily enough from a flownet.

   Problems of undrained behaviour during excavation can also be tackled using mobilized shear strength c_{mob} directly (Bolton, Powrie and Stewart 1987).

5. CONCLUSIONS

1. It has been demonstrated that centrifuge model tests can form the basis of research into soil-structure interaction. It is necessary to simplify the complex of data which is obtained by imposing upon it certain idealisations which caricature the essential behaviour patterns. Such caricatures can lead to the enrichment of engineering design calculations.

   Experimental techniques do need to be refined, however. Problems of mis-fit of stiff soil against relatively stiff structures were found to limit the capacity of the experimenter to exercise fine control over kinematic boundary conditions. Methods of grouting and excavation in-flight will have to be developed if more difficult problems are to be researched with greater precision and control.

2. The adoption of geostructural mechanisms in this paper has followed the spirit of engineers' beam theory. Beam theory neglects shear deformations in favour of a simple mechanistic treatment of bending in terms of plane sections remaining plane. Although "wrong", engineers' beam theory proves more useful to the designer than more complete approaches, since it characterises stress and strain in a consistent fashion which is geometrically simple. Experiment proves it to be acceptably accurate for a particular class of beams which are "slender".

   Designers facing difficulties with soil-structure interaction have suffered from a lack of such simplified treatments. Code formulae have often been based on poorly digested information peculiar to a given site, which should not have been applied in other contexts. On the other hand, finite element analyses produce such a volume of detailed prediction that patterns are difficult to discern and assumptions - especially of the material stress-strain laws - difficult to evaluate.

   It is proposed that geostructural mechanisms which are based on "lower bound" stress fields, but which incorporate consistent strain fields, are a suitable design tool. In the present work it has been demonstrated that any desired stress-strain relation could have been used as the basis of prediction, though the technique should naturally lead to the adoption of real data from stress paths appropriate to the problem. Such proposed mechanisms must, of course, be tested. The centrifuge model technique appears well suited to this task.

3. Centrifuge tests which are intended to support the designer must address those situations which can be forseen to be critical in the construction and life of the structure. In this sense, the test environment must be as harsh as it could possibly be in reality. Sometimes, the harshest possible combination of influences is not immediately obvious and must itself be subject to experimental enquiry. In the sequence of tests reported here the groundwater conditions selected for design are of paramount significance. It has been found that free water can suddenly destabilize temporary walls which have not been adequately propped. The behaviour of walls embedded in clays with deep or shallow water tables has been shown to be utterly different; and the most damaging bending moments have been found to exist in well-propped walls in de-watered clays which have then been subjected to an episode of rising groundwater pressures (Bolton, Powrie and Stewart 1987).

   It is essential that appropriate limit state events are studied in centrifuge model tests, and that sufficient thought is given in advance of testing to those events. No subsequent re-interpretation can remedy the situation if the tests are inadequately planned.

ACKNOWLEDGEMENT

The first author of this paper was employed by the University of Cambridge. The work reported herein was carried out under a contract placed on him by the Transport and Road Research Laboratory. The views expressed are not necessarily those of the Department of Transport.

The second author received support from the Science and Engineering Research Council.

The third author was employed by the University of Cambridge.

REFERENCES

Al-Tabbaa, A. 1987. Unpublished, forthcoming Ph.D. Thesis, Cambridge University.

Bolton, M.D. & Powrie, W. 1987. The collapse of diaphragm walls retaining clay. Geotechnique 37, No.3.

Bolton M.D, Powrie W, & Stewart D.I. 1987 Effects on diaphragm walls of ground-water pressure rising in clays. Proc. 9th Eur. Conf. Soil Mech. & Found. Eng., Dublin, V2, 759-762

Bransby, P.L. & Milligan, G.W.E. 1975. Soil deformations near cantilever sheet-pile walls. Geotechnique 25, No.2, p175-195.

Powrie W. 1986. The behaviour of diaphragm walls in clay. Ph.D. Thesis, Cambridge University.

Schofield A.N. 1980. Cambridge geotechnical centrifuge operations. Geotechnique 30, No.3, p225-268.

Sketchley C.J. 1973. Behaviour of kaolin in plane strain. Ph.D. Thesis, Cambridge University.

White T.P. 1987. Finite element calculations involving the yielding of dilatant soils. M. Phil. Thesis, Cambridge University.

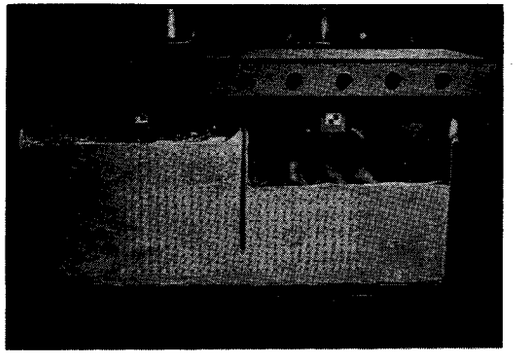

Figure 1 Typical model (DWC07) ready for testing

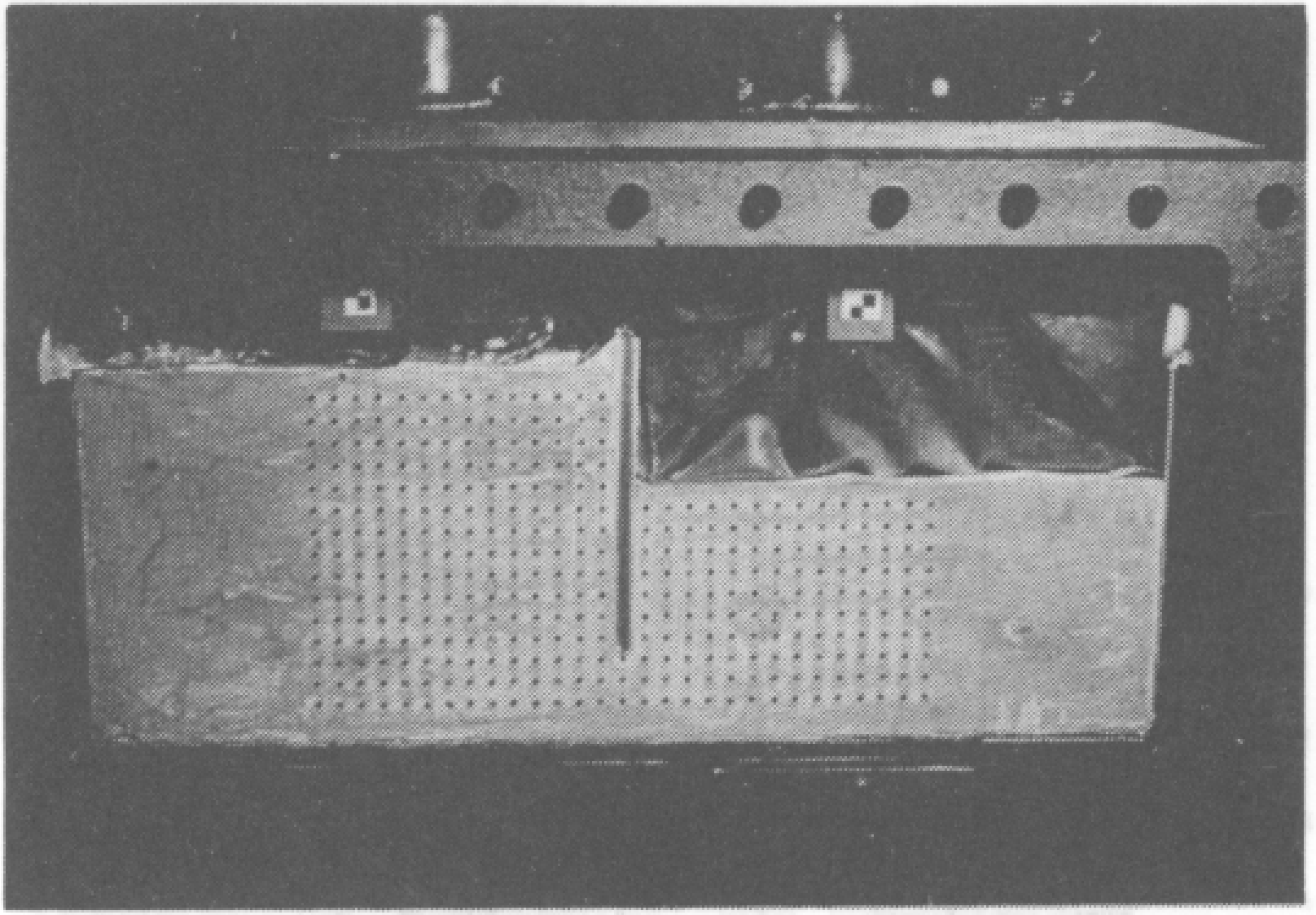

Figure 1 Typical model (DWC07) ready for testing

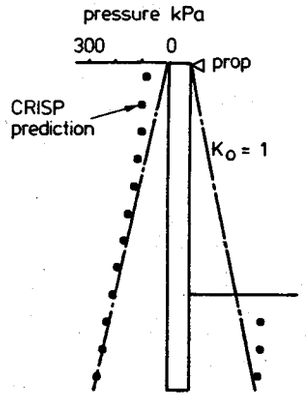

Figure 2 Lateral pressures prior to "excavation"

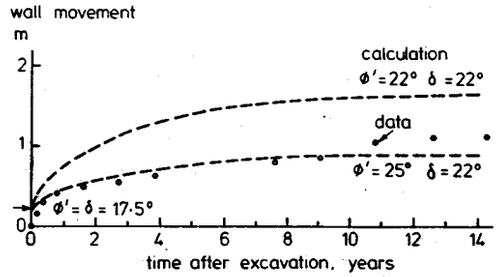

Figure 4 Scaled crest deflections, DWC08

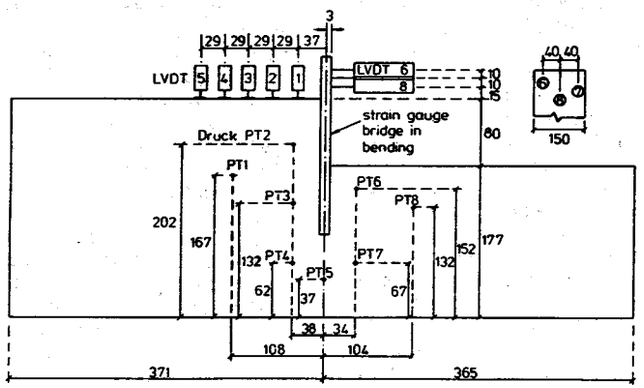

Figure 3 Instrumentation of a typical model

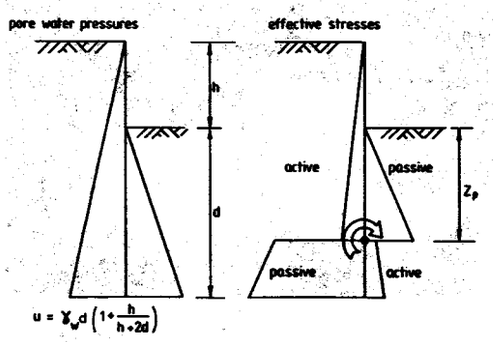

Figure 5 Equili brium stress analysis for an unpropped wall

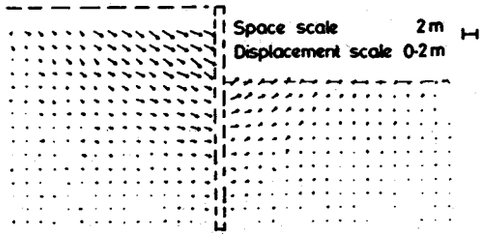

Figure 6 Soil displacements measured during "excavation" phase, DWC08

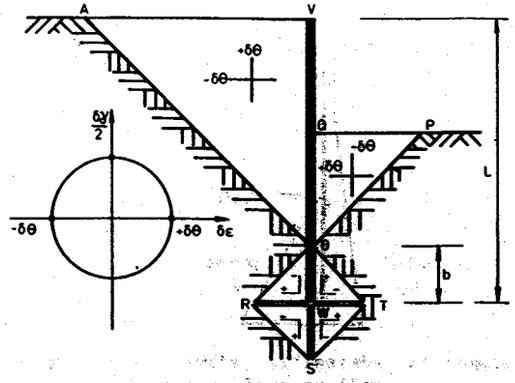

Figure 7 Admissible strain field for unpropped wall

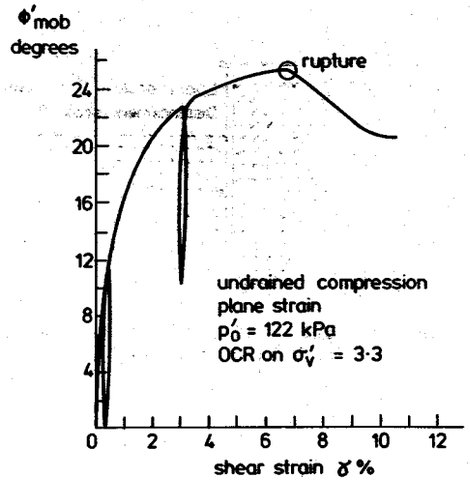

Figure 8 Mobilised angle of shearing

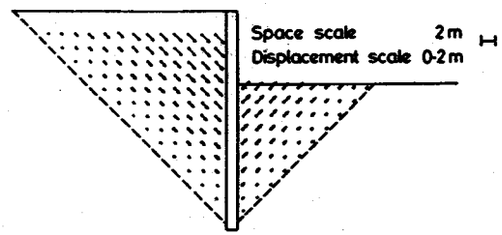

Figure 9 Soil displacements calculated for "excavation" phase, DWC08

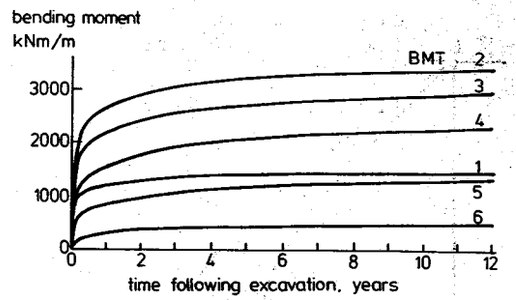

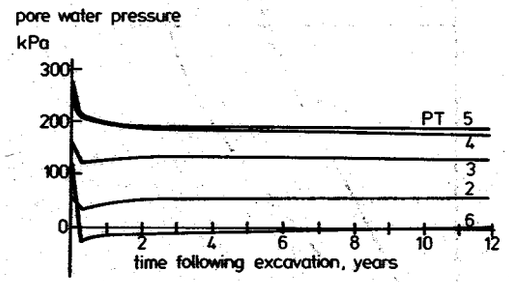

Figure 10 Transient response at prototype scale, DWC16

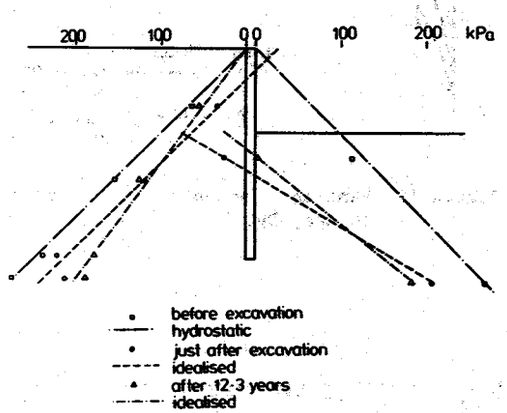

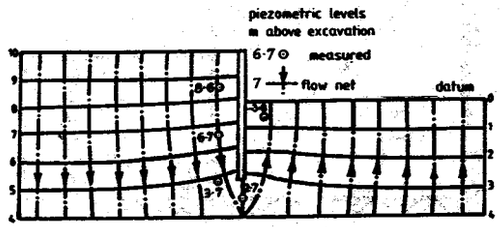

Figure 11 Pore water pressures, DWC16

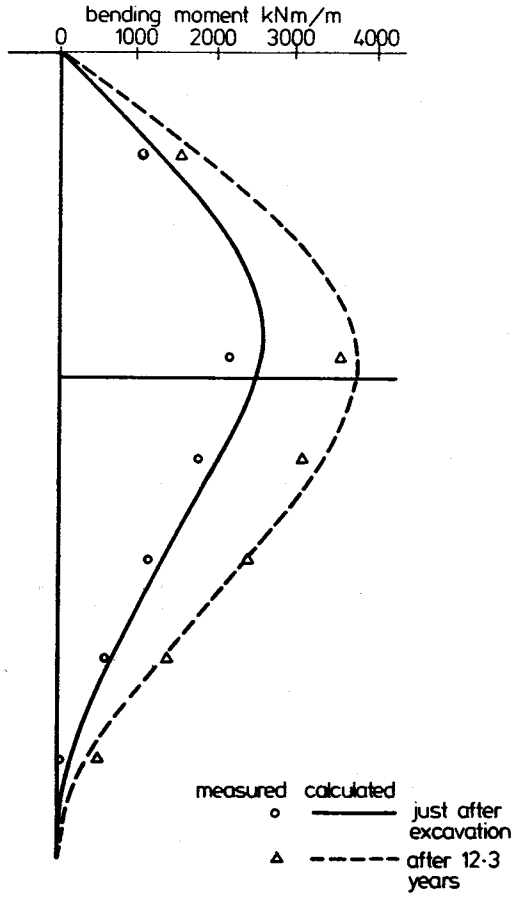

Figure 12 Bending moments and prop forces, DWC16

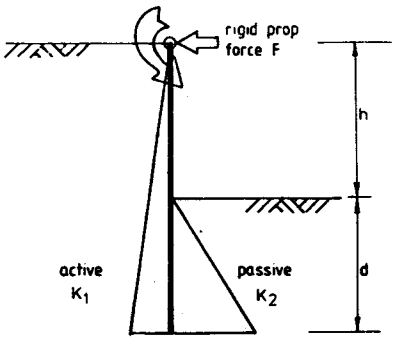

Figure 14 Admissible stress field for wall propped at crest

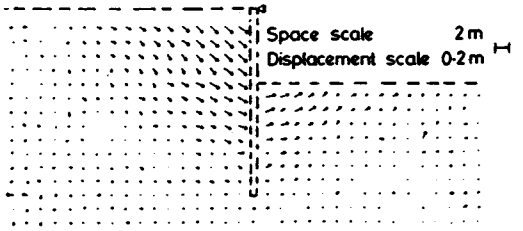

Figure 15 Soil displacements during excavation, test DWC16

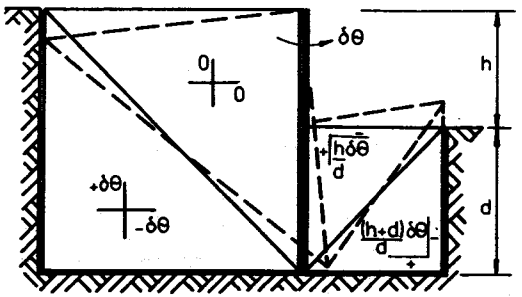

Figure 13 Admissible strain field for embedded wall, rotating about crest

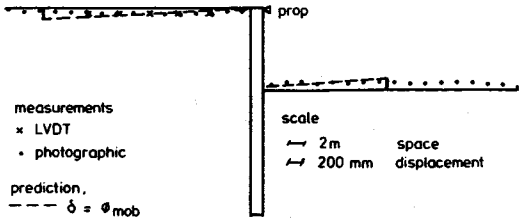

Figure 16 Measured and calculated settlements, DWC14